NeuroImage: Clinical 17 (2018) 530–540

Contents lists available at ScienceDirect

NeuroImage: Clinical

journal homepage: www.elsevier.com/locate/ynicl

Iron-related gene variants and brain iron in multiple sclerosis and healthy individuals

Jesper Hagemeier[a,*], Murali Ramanathan[b], Ferdinand Schweser[a,c], Michael G. Dwyer[a], Fuchun Lin[a], Niels Bergsland[a], Bianca Weinstock-Guttman[d], Robert Zivadinov[a,c]

[a] Buffalo Neuroimaging Analysis Center, Department of Neurology, Jacobs School of Medicine and Biomedical Sciences, University at Buffalo, The State University of New York, Buffalo, NY, USA
[b] Department of Pharmaceutical Sciences, School of Medicine and Biomedical Sciences, State University of New York, Buffalo, NY, USA
[c] Center for Biomedical Imaging, Clinical and Translational Science Institute, Jacobs School of Medicine and Biomedical Sciences, University at Buffalo, The State University of New York, Buffalo, NY, USA
[d] Jacobs Multiple Sclerosis Center, Department of Neurology, Jacobs School of Medicine and Biomedical Sciences, University at Buffalo, The State University of New York, Buffalo, NY, USA

ARTICLE INFO

Keywords:
Iron related genes
Quantitative susceptibility mapping
QSM
Iron
Multiple sclerosis

ABSTRACT

Brain iron homeostasis is known to be disturbed in multiple sclerosis (MS), yet little is known about the association of common gene variants linked to iron regulation and pathological tissue changes in the brain. In this study, we investigated the association of genetic determinants linked to iron regulation with deep gray matter (GM) magnetic susceptibility in both healthy controls (HC) and MS patients. Four hundred (400) patients with MS and 150 age- and sex-matched HCs were enrolled and obtained 3 T MRI examination. Three (3) single nucleotide polymorphisms (SNPs) associated with iron regulation were genotyped: two SNPs in the human hereditary hemochromatosis protein gene *HFE*: rs1800562 (C282Y mutation) and rs1799945 (H63D mutation), as well as the rs1049296 SNP in the transferrin gene (C2 mutation). The effects of disease and genetic status were studied using quantitative susceptibility mapping (QSM) voxel-based analysis (VBA) and region-of-interest (ROI) analysis of the deep GM. The general linear model framework was used to compare groups. Analyses were corrected for age and sex, and adjusted for false discovery rate. We found moderate increases in susceptibility in the right putamen of participants with the C282Y (+6.1 ppb) and H63D (+6.9 ppb) gene variants vs. non-carriers, as well as a decrease in thalamic susceptibility of progressive MS patients with the C282Y mutation (left: −5.3 ppb, right: −6.7 ppb, $p < 0.05$). Female MS patients had lower susceptibility in the caudate (−6.0 ppb) and putamen (left: −3.9 ppb, right: −4.6 ppb) than men, but only when they had a wild-type allele ($p < 0.05$). Iron-gene linked increases in putamen susceptibility (in HC and relapsing remitting MS) and decreases in thalamus susceptibility (in progressive MS), coupled with apparent sex interactions, indicate that brain iron in healthy and disease states may be influenced by genetic factors.

1. Introduction

In the brain, iron is an abundant element mostly stored in ferritin clusters. It is essential for brain development and is involved in many biochemical processes, including myelin synthesis (Hagemeier et al., 2012a; Rouault, 2013). In several neurological disorders such as multiple sclerosis (MS), brain iron is dysregulated and often present around plaques as activated iron-laden macrophages (Mehta et al., 2013; Haider et al., 2014). Excessive free iron in the deep gray matter (GM) may induce (e.g. due to oligodendrocyte dysfunction) or amplify neurodegeneration through generation of reactive oxygen species (Farina et al., 2013).

Brain iron concentrations have long been known to increase with normal aging (Hallgren and Sourander, 1958; Hagemeier et al., 2017). In most deep GM regions, the increase appears to slow down and level with age, while in the thalamus a reduction in iron concentration is

Abbreviations: MS, multiple sclerosis; GM, gray matter; HFE, human hemochromatosis gene; QSM, quantitative susceptibility mapping; HC, healthy control; RRMS, relapsing-remitting multiple sclerosis; EDSS, Expanded Disability Status Scale; TF, transferrin; SNP, single nucleotide polymorphism; GRE, gradient recalled echo; T1w, T1-weighted; ppb, parts per billion; VBA, voxel-based analysis; TFCE, threshold-free cluster enhancement; FWE, family-wise error rate; GLM, general linear model; FDR, false discovery rate; ROI, region of interest; MSSS, multiple sclerosis severity scale

* Corresponding author at: Buffalo Neuroimaging Analysis Center, Department of Neurology, University at Buffalo, 100 High St., Buffalo, NY 14203, USA.
E-mail address: jhagemeier@bnac.net (J. Hagemeier).

https://doi.org/10.1016/j.nicl.2017.11.003
Received 21 August 2017; Received in revised form 1 November 2017; Accepted 3 November 2017
Available online 08 November 2017

often observed after mid-life. Also, sex differences have been reported (Bartzokis et al., 2010), with men having higher brain iron loads. For years, many post-mortem and in vivo studies using iron-sensitive imaging techniques have described changes in brain iron homeostasis in an array of neurologic disorders (Hagemeier et al., 2012a; Ward et al., 2014), including Alzheimer's disease (Jellinger et al., 1990; Connor et al., 1992; Acosta-Cabronero et al., 2013), Parkinson's disease (Jellinger et al., 1990; Costa-Mallen et al., 2017), and MS (Craelius et al., 1982; Zivadinov et al., 2012; Hagemeier et al., 2017).

Genetic variations in iron-regulating genes, e.g., H63A and C282Y variants of the human hemochromatosis (*HFE*) gene, can influence peripheral iron load (Burt et al., 1998). However, it remains unclear to what extent specific iron-regulating genes influence brain iron homeostasis, and whether there would be effects specific to neurological diseases. A recent R2* study by Pirpamer et al. (Pirpamer et al., 2016) did not observe iron regulatory gene effects (nor any effect of sex) on brain iron levels of healthy subjects. Another study, however, reported that healthy men carrying either the *HFE* or Transferrin C2 genetic variant did have increased caudal iron levels, as compared to non-carriers (Bartzokis et al., 2010), suggesting that a genetic effect on brain iron may be sex dependent. Iron gene status may also be linked to the association between brain iron and cognition (Bartzokis et al., 2011). In addition, the presence of common gene variants involved in iron metabolism and transport appear to influence the age of onset and disease severity, and are more prevalent in neurological diseases associated with iron dysregulation, such as Alzheimer's disease (van Rensburg et al., 1993; Moalem et al., 2000; Sampietro et al., 2001), amyotrophic lateral sclerosis (Wang et al., 2004), and Parkinson's disease (Dekker et al., 2003). In two European MS studies, the frequency of *HFE* H63A and C282Y variants were comparable to controls. However, *HFE* C282Y mutant allele carriers did report earlier disease onset (Ristic et al., 2005) and more rapid disability progression (Bettencourt et al., 2011). An Australian study reported increased prevalence of the *HFE* C282Y mutation in MS (10.2% vs. controls: 6.7%) (Rubio et al., 2004).

In MS, studies have shown that brain iron levels are disturbed especially in the deep GM (Bakshi et al., 2002; Zivadinov et al., 2012; Stankiewicz et al., 2014), and around plaques (Craelius et al., 1982). Several recent MRI studies have utilized the novel quantitative susceptibility mapping (QSM) technique in MS to investigate in vivo tissue changes (Zhang et al., 2016; Hagemeier et al., 2017). QSM is an advanced MR imaging method (Reichenbach et al., 2015; Schweser et al., 2016) allowing the measurement of subtle changes of the magnetic susceptibility, reflecting tissue concentrations of paramagnetic iron complexes (Langkammer et al., 2012; Stuber et al., 2014), but also calcium (Schweser et al., 2010; Chen et al., 2014; Stuber et al., 2014), and myelin (Schweser et al., 2011; Stuber et al., 2014; Groeschel et al., 2016). It is currently regarded as one of the most sensitive and specific techniques for studying tissue iron in vivo (Langkammer et al., 2013; Stuber et al., 2015).

To date, gene variants linked to iron regulation have not been investigated in the context of in vivo brain iron measurements in MS patients. As such, the present study investigated the effect of genetic variants linked to iron regulation in relation to deep GM tissue changes as measured by QSM in both healthy individuals and MS patients.

2. Methods

2.1. Subjects

In this substudy of the cardiovascular, genetic and environmental study in MS (Kappus et al., 2016; Zivadinov et al., 2016), healthy controls (HC) and MS patients were prospectively enrolled and group-matched by age and sex: 150 HC and 400 MS patients (relapsing-remitting [RRMS]: 261, progressive MS: 139). Subjects needed to have 3 T MRI examination with the sequences suitable for QSM and brain volumetry examination having been applied successfully, as well as genetic determination for iron-related gene variants. MS patients were included if they had a relapsing or progressive (secondary- or primary-progressive) disease course. Patients with a relapse and/or steroid treatment within 30 days prior to MRI were excluded. Additional exclusion criteria were: pregnancy, presence of pre-existing medical conditions known to be associated with brain pathology (e.g., cerebrovascular disease, positive history of alcohol dependence). MS patients were diagnosed using the revised McDonald criteria (Polman et al., 2011) and clinical disease severity was measured using the Expanded Disability Status Scale (EDSS) (Kurtzke, 1983). HC were recruited from volunteers with a normal neurological examination and no history of neurologic disorders or chronic psychiatric disorders. The study was approved by the local Institutional Review Board at the University at Buffalo. Written informed consent was obtained from all participants.

2.2. Genotyping

Anti-coagulated peripheral blood was obtained by venipuncture for all participants. DNA was extracted from peripheral blood mononuclear cells preserved in TRI reagent (Molecular Research Center Inc., Cincinnati, OH, USA). A panel of candidate single nucleotide polymorphisms (SNPs) linked to iron regulation pathways were genotyped using the OpenArray platform (Applied Biosystems, Life Technologies, Foster City, CA). The genotyped polymorphisms were: rs1800562, rs1799945, and rs1049296. The SNP rs1800562 is found in the majority of cases with hemochromatosis (risk allele A: C282Y). The SNP rs1799945 is also a gene associated with hereditary hemochromatosis (risk allele G: H63D). rs1049296 is associated with transferrin (TF), the main iron transport protein (risk allele T: C2-subtype). The homozygous and heterozygous minor allele-containing genotypes (classified as ‘carriers’) were pooled for statistical comparison to the homozygous major allele genotype (classified as ‘non-carriers’).

2.3. MRI image acquisition

All participants were imaged with the same clinical 3 T GE Signa Excite HD 12.0 scanner (General Electric, Milwaukee, WI, USA) using an eight-channel head-and-neck coil. A detailed description of pulse sequences and image reconstruction steps has been reported previously (Hagemeier et al., 2017). Briefly, acquired sequences included a 3D single-echo spoiled gradient recalled echo (GRE) sequence for QSM (512x192x64 matrix and a nominal resolution of $0.5 \times 1 \times 2\ mm^3$ (FOV = $256 \times 192 \times 128\ mm^3$), flip angle = 12°, TE/TR = 22 ms/40 ms, and bandwidth = 13.89 kHz) and a 3D T1-weighted (T1w) fast spoiled GRE sequence for the determination of brain volume measures (TE/TI/TR = 2.8/900/5.9 ms, flip angle = 10°, isotropic 1 mm resolution).

2.4. QSM

QSM processing was performed by a fully automated pipeline with in-house developed MATLAB programs (2013b, The MathWorks, Natick, MA). Processing and susceptibility map reconstruction details were provided previously (Hagemeier et al., 2017). Magnitude and phase GRE images were reconstructed offline on a $512 \times 512 \times 64$ spatial matrix. *K*-space was zero-padded in phase-encode direction prior to the processing to achieve isotropic in-plane resolution. Distortions due to imaging gradient non-linearity were compensated (Polak et al., 2015). Phase images were unwrapped with a best-path algorithm (Abdul-Rahman et al., 2007), background-field corrected with V-SHARP (Schweser et al., 2011; Wu et al., 2012) (radius 5 mm; TSVD threshold 0.05), and converted to magnetic susceptibility maps using the HEIDI algorithm (Schweser et al., 2012). Magnetic susceptibility maps were referenced (0 ppb) to the average susceptibility of the brain. This was done to minimize potential confounding bias from

Table 1
Clinical and demographic data.

	HC n = 150	Multiple sclerosis (n = 400)	p-value
Female, n (%)	99 (66%)	256 (64%)	0.662
Age	45.6 (12.9)	46.6 (10.5)[b]	0.400
Relapsing-remitting MS, n (%)	n/a	261 (65%)	n/a
Progressive MS, n (%)	n/a	139 (35%)[c]	n/a
EDSS, median ± IQR	n/a	3.0 (2.0–5.5)	n/a
Disease duration in years	n/a	14.8 ± 10.7	n/a
Relapses in the previous year, median ± IQR	n/a	0 ± (0–1)	n/a
Age of MS onset, mean (SD)	n/a	32.0 (9.8)	n/a
Disease modifying therapy, n (%)			
Non-therapy	n/a	113 (28%)	n/a
Interferons	n/a	112 (28%)	
Glatiramer acetate	n/a	72 (18%)	
Natalizumab	n/a	49 (12%)	
Immunosuppressant	n/a	5 (1%)	
Combination therapy	n/a	4 (1%)	
Other/unknown	n/a	45 (11%)	
HFE rs1800562 A allele[a]	13 (9%)	47 (12%)	0.331
HFE rs1799945 G allele[a]	34 (23%)	115 (29%)	0.136
TF rs1049296 T allele[a]	26 (17%)	117 (29%)	0.005

Note: n/a; not applicable; HC: healthy control; EDSS = Expanded Disability Status Scale. HFE = human hemochromatosis, TF = transferrin.
[a] Number of risk-allele carriers either heterozygous and homozygous. The number of heterogeneous carriers were: HC = 0, MS = 0 for rs1800562 A allele, HC = 6, MS = 11 for rs1799945 G allele, HC = 1, MS = 11 for rs1049296 T allele.
[b] Mean (SD) age of RRMS and progressive MS: 43.0 (10.1), 52.8 (7.7).
[c] SPMS: n = 102, PPMS: n = 37.

(unknown) disease-related susceptibility changes, e.g. due to demyelination, in a more localized anatomical reference region (Deistung et al., 2013; Straub et al., 2017), as well as limit the inter-subject variability resulting from an absolute reference susceptibility value. Magnetic susceptibility is reported in parts per billion (ppb).

2.5. Voxel-based analysis

We performed a voxel-based analysis (VBA) of the susceptibility maps to determine SNP and disease-related tissue alterations without prior assumptions about the location of the changes. To this end, susceptibility maps were normalized with the diffeomorphic Greedy-SyN transformation model (Advanced Normalization Tools; version 2.1; http://stnava.github.io/ANTs) to an in-house generated susceptibility brain template created from 90 subjects (30 HC, 30 RRMS, and 30 secondary progressive patients over a wide range of ages) with 1 mm^3 isotropic voxel size (Hanspach et al., 2017).

After smoothing with a 1 mm Gaussian kernel, we performed voxel-wise statistical analysis via non-parametric permutation tests (FSL randomise (Winkler et al., 2014); 5000 permutations) using age and sex as covariates to identify susceptibility differences between patient groups and their respective control groups. Both analyses with and without threshold-free cluster enhancement (TFCE) controlling for family-wise error (FWE) rate, were carried out at the $p < 0.05$ level.

2.6. Deep gray matter segmentation

Anatomical deep GM regions were segmented using FSL FIRST (http://fsl.fmrib.ox.ac.uk/fsl/fslwiki/FIRST (Patenaude et al., 2011)) on 3D SPGR T_1w images corrected for T_1-hypointensity misclassification (Gelineau-Morel et al., 2012). Mean values of susceptibility were calculated in bilateral thalamus, caudate, putamen, and globus pallidus. To obtain the tissue volume of each region, volumes were normalized to the participants' head volume as determined by the SIENAX-derived scaling factor (FMRIB SIENAX version 2.6) (Smith et al., 2002). Volumes are expressed in milliliters.

2.7. Statistical analysis

Analyses were carried using SPSS 24.0 (IBM, Armonk, NY) and R (3.2.1, R Foundation for Statistical Computing, Vienna, Austria). Normality of distributions was tested using Q-Q plots and the Shapiro-Wilk test. Baseline characteristics were compared using chi-squared and Student's *t*-test. Paired student's *t*-test was used to determine whether mean values of anatomical regions were different between left and right hemispheres. Outcome measures were averaged between left and right hemispheres in case no significant hemisphere effect was observed; otherwise analyses were carried out separately. Main effects of disease, MS course, age, sex and carrier status on magnetic susceptibility were analyzed using student *t*-test and Spearman's rank correlation analysis. Magnetic susceptibility and volume of the carriers and non-carrier groups were explored within the general linear model (GLM) framework between disease and MS course, with all models including age, age^2, and sex terms. Analyses split by sex were adjusted for age. Because changes in susceptibility in MS could be driven by loss of tissue (Hagemeier et al., 2017), post-hoc analyses corrected for the structural volume in question were carried out when a significant difference in magnetic susceptibility was observed. Clinical associations of genotypes were assessed with EDSS using the Mann-Whitney *U* test. Effect sizes were estimated with Cohen's *d*, α-level was set at 0.05, and significance levels are reported both as uncorrected ($p < 0.05$) and corrected for multiple comparisons using false discovery rate (FDR; q-value < 0.05) (Benjamini and Hochberg, 1995), in order to both maximize statistical power, minimize false negative findings, while also reporting stringent p-value correction.

3. Results

3.1. Clinical, demographic and genotype characteristics

The distribution of age and sex between control subjects (45.6 ± 12.9 years, 66% female) and MS patients (46.6 ± 10.5 years, 64% female) was highly similar ($p = 0.400$ and $p = 0.662$, respectively) (Table 1). Among MS patients, the median EDSS score was 3.0 (IQR: 2.0–5.5), disease duration was 14.8 ± 10.7 years, and 65.3% had a relapsing disease course (RRMS).

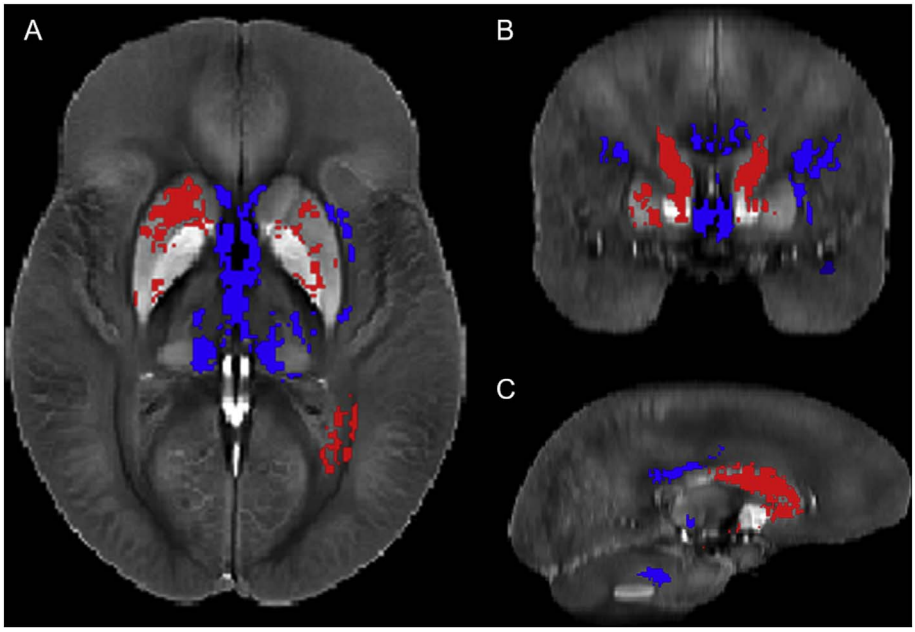

Fig. 1. Results of the Voxel Based Analysis (VBA) for non-carrier MS patients vs. controls shown in the (a) axial, (b) coronal, and (c) sagittal plane. Shown are voxels with a p-value below 0.05 after FWE correction with TFCE in selected slices. Red indicates voxels where MS > HC (putamen; $p < 0.05$), blue indicates voxels where HC > MS (thalamus, medial pulvinar nucleus; $p < 0.05$). (For interpretation of the references to color in this figure legend, the reader is referred to the web version of this article.)

The proportions of risk allele carriers of rs1800562 (C282Y) and rs1799945 (H63D) were similar between the two study groups ($p = 0.331$ and $p = 0.136$); however, MS patients had a significantly increased frequency of rs1049296 T allele carriers (TF-C2; 17% vs. 29%, $p = 0.005$). There were no significant differences in demographic characteristics between risk-allele carriers and non-carriers.

3.2. Voxel based analysis

Fig. 1 shows the regions with significantly different susceptibility values between MS patients with non-carrier alleles and HCs when using TFCE. MS patients had a statistically significant higher susceptibility in the putamen and caudate, especially in the right hemisphere ($p < 0.05$). Thalamic susceptibility was significantly lower in MS patients, predominantly in the medial pulvinar nucleus of the thalamus. VBA analysis of the C282Y, H63D, and C2 gene variants did not reveal strong effects, although findings were significant in analyses without TFCE-FWE adjustments (see Supplement 1 and Supplement Fig. 1).

To further investigate the relationship between allele status and study group effects, stratified GLM analyses were carried out.

3.2.1. Main effects of study groups, age, sex, and carrier status on magnetic susceptibility

Hemispheric differences of susceptibility were observed in region of interest (ROI) analyses of the thalamus (right + 1.4 ppb, $p < 0.001$), putamen (right + 2.8 ppb, $p < 0.001$), and pallidus (right + 2.5 ppb, $p < 0.001$), but not the caudate (right − 0.5 ppb, $p = 0.301$). Subsequent analyses were split by hemisphere for the thalamus, putamen and pallidus.

Main effects of study group are presented in Supplement Table 1. MS patients had higher susceptibility than HC in the caudate (+ 7.5 ppb, $p < 0.001$), left and right putamen (left: + 2.9 ppb, $p = 0.042$; right: + 4.2 ppb, $p = 0.007$) and left and right pallidus (left: + 14.8 ppb, $p < 0.001$; right: + 15.1 ppb, $p < 0.001$), while left and right thalamus susceptibility was markedly lower in MS (left: − 6.8 ppb, $p < 0.001$; right: − 6.1 ppb, $p < 0.001$). Compared to RRMS, progressive patients had higher susceptibility in the caudate (+ 2.7 ppb, $p = 0.026$), right putamen (+ 4.4 ppb, $p = 0.011$), right pallidus (+ 6.4 ppb, $p = 0.029$), and lower susceptibility in the bilateral thalamus (left: − 3.1 ppb, $p = 0.002$; and right: − 2.7 ppb, $p = 0.009$).

Using the total sample, iron risk allele status was not associated with change in susceptibility, except for H63D carriers having higher left and right putamen susceptibility (left: + 4.0 ppb, $p = 0.006$ and right: + 3.5 ppb, $p = 0.024$). Within both HC and MS, age was associated with susceptibility (between $r = 0.170–0.430$, $p < 0.05$), except in the right thalamus of HCs ($r = -0.147$, $p = 0.074$, likely due to a non-linear age progression of thalamic susceptibility). Sex differences were observed in the caudate (HC: 3.6 ppb, $p = 0.043$ and MS: + 5.5 ppb, $p < 0.001$), with men having higher susceptibility. All significant main effects, except sex differences within HCs, remained after adjusting for FDR ($q < 0.05$).

3.2.2. Magnetic susceptibility and carrier status stratified by group

To investigate possible interaction effects, stratified analyses were carried out. Within controls, C282Y risk allele carriers had higher right-sided putamen susceptibility (+ 6.1 ppb, $d = 0.53$, $p = 0.040$; Table 2), although significance was lost after FDR correction. Similarly, HC H63D carriers had higher right putamen susceptibility (+ 6.7 ppb, $d = 0.44$, $p = 0.039$). Within MS, an effect was observed in the left putamen (+ 3.2 ppb, $d = 0.21$, $p = 0.040$). All group-wise analyses, except some of the comparisons within the putamen, yielded significant results indicating differences between controls and MS patients ($p < 0.05$, $q < 0.05$; Table 2).

Volumetric comparisons are presented in Supplement Material 2 and Supplement Table 2. To determine whether the observed susceptibility differences of HCs in the left (H63D) and right (C282Y and H63D) putamen (Table 2) were independent from volumetric effects, structural volume was added as covariate. Effects remained significant after this correction (Tables 2 & 3).

3.2.3. Magnetic susceptibility associated with carrier status stratified by MS type

Analyses stratified by MS type are shown in Table 3. Within progressive MS, C282Y risk-allele carriers had lower thalamic susceptibility (left: − 5.3 ppb, $d = 0.56$, $p = 0.043$, right − 6.7 ppb, $d = 0.62$, $p = 0.007$, Fig. 2), an effect that remained significant after adjusting for thalamic volume. Additionally, left putamen susceptibility was higher among relapsing H63D risk-allele carriers (+ 5 ppb, $d = 0.33$, $p = 0.047$). Adjustment for FDR resulted in loss of significance.

Table 2
Mean magnetic susceptibility (in ppb) of risk allele carriers and non-carriers among healthy controls and patients with multiple sclerosis.

HFE rs1800562 (C282Y)

	HC			MS			Overall p-value
	Non-carrier	Carrier	p-value (*d*)	Non-carrier	Carrier	p-value (*d*)	
T Thalamus							
L Thalamus	− 1.4 (7.0)	0.5 (6.9)	0.637 (0.27)	− 7.8 (9.3)	− 9.6 (10.6)	0.163 (0.18)	< **0.001**[*,†]
R Thalamus	− 0.4 (7.1)	2.8 (7.3)	0.173 (0.44)	− 6.2 (9.3)	− 7.7 (10.8)	0.235 (0.15)	< **0.001**[*,†]
T Caudate	36.7 (10.1)	35.6 (9.8)	0.650 (0.11)	44.9 (11.7)	43.0 (12.1)	0.463 (0.16)	< **0.001**[*,†]
L Caudate							
R Caudate							
T Putamen							
L Putamen	46.1 (14.6)	51.3 (14.1)	0.073 (0.36)	50.2 (15.5)	48.9 (13.9)	0.730 (0.09)	0.121
R Putamen	47.7 (15.9)	53.8 (3.3)	**0.040**[*] **(0.53)**	53.7 (16.2)	51.1 (15.1)	0.388 (0.17)	**0.010**[*,†]
T Pallidus							
L Pallidus	112.5 (22.1)	109.1 (23.9)	0.754 (0.15)	127.6 (25.5)	124.8 (27.0)	0.586 (0.11)	< **0.001**[*,†]
R Pallidus	104.3 (21.9)	103.2 (14.0)	0.999 (0.06)	119.8 (26.7)	117.9 (25.6)	0.717 (0.07)	< **0.001**[*,†]

HFE rs1799945 (H63D)

	HC			MS			Overall p-value
	Non-carrier	Carrier	p-value (*d*)	Non-carrier	Carrier	p-value (*d*)	
T Thalamus							
L Thalamus	− 0.5 (7.0)	− 3.1 (6.9)	0.063 (0.37)	− 7.7 (9.2)	− 8.6 (10.0)	0.317 (0.09)	< **0.001**[*,†]
R Thalamus	− 0.1 (7.3)	− 0.2 (6.4)	0.944 (0.01)	− 6.2 (8.7)	− 6.6 (11.0)	0.622 (0.04)	< **0.001**[*,†]
T Caudate	36.1 (8.9)	38.3 (12.9)	0.393 (0.20)	44.3 (12.0)	45.3 (11.2)	0.346 (0.09)	< **0.001**[*,†]
L Caudate							
R Caudate							
T Putamen							
L Putamen	45.3 (14.7)	50.9 (13.5)	0.058 (0.40)	49.1 (14.9)	52.3 (15.8)	**0.040**[*] (0.21)	**0.020**[*,†]
R Putamen	46.7 (15.4)	53.6 (15.9)	**0.039**[*] **(0.44)**	52.7 (16.2)	54.8 (15.7)	0.213 (0.13)	**0.010**[*,†]
T Pallidus							
L Pallidus	112.4 (22.4)	110.5 (21.5)	0.639 (0.09)	126.4 (24.8)	128.7 (27.1)	0.639 (0.09)	< **0.001**[*,†]
R Pallidus	103.5 (20.9)	104.6 (21.9)	0.701 (0.05)	119.3 (26.9)	119.2 (25.4)	0.993 (0.01)	< **0.001**[*,†]

TF rs1049296 (TF-C2)

	HC			MS			Overall p-value
	Non-carrier	Carrier	p-value (*d*)	Non-carrier	Carrier	p-value (*d*)	
T Thalamus							
L Thalamus	− 1.5 (7.3)	0.1 (5.9)	0.100 (0.24)	− 8.3 (9.5)	− 7.0 (9.1)	0.245 (0.14)	< **0.001**[*,†]
R Thalamus	− 0.1 (7.3)	− 1.1 (6.8)	0.708 (0.14)	− 6.5 (9.1)	− 6.0 (9.8)	0.679 (0.05)	< **0.001**[*,†]
T Caudate	37.5 (10.8)	35.8 (9.5)	0.175 (0.1)	44.0 (10.7)	45.6 (11.6)	0.571 (0.14)	< **0.001**[*,†]
L Caudate							
R Caudate							
T Putamen							
L Putamen	48.1 (15.4)	44.6 (13.7)	0.069 (0.24)	50.1 (15.8)	50.4 (13.3)	0.963 (0.02)	0.285
R Putamen	49.9 (16.8)	46.6 (12.8)	0.117 (0.22)	52.9 (16.2)	53.9 (14.5)	0.542 (0.07)	0.089
T Pallidus							
L Pallidus	112.0 (21.4)	113.7 (23.7)	0.927 (0.08)	128.2 (26.3)	124.3 (23.6)	0.154 (0.16)	< **0.001**[*,†]
R Pallidus	103.5 (21.4)	108.5 (18.3)	0.734 (0.25)	120.4 (27.8)	116.5 (26.5)	0.220 (0.14)	< **0.001**[*,†]

Note: HC = Healthy Control; MS = Multiple Sclerosis; T = Total; L = Left; R = Right. $p < 0.05$ and Cohen's *d* medium effect (> 0.50) are bolded.
Thalamus, putamen and pallidus analyses were carried out separately for the left and right hemisphere due to observed hemispheric differences.
[*] Remains significant ($p < 0.05$) after adjusting for structural volume.
[†] Remains significant ($q < 0.05$) after FDR correction by gene.

3.2.4. Susceptibility between male and female MS patients stratified by carrier status

Women had consistently lower susceptibility in the caudate and putamen ($d = 0.26$–0.59, $p < 0.001$–0.049), but only among patients who did not carry risk alleles, regardless of SNP (Table 4). Male risk-allele carriers had similar, or slightly lower (higher for thalamus), susceptibilities as compared to male non-carriers (all $p \geq 0.120$). Female risk-allele carriers, however, had overall higher (lower for thalamus) susceptibilities than female non-carriers (H63D carriers vs. non-carriers: left putamen $p = 0.024$, right putamen $p = 0.010$, all others $p \geq 0.071$), bringing them in line with males. Female *TF*-C2 risk-allele carriers had even lower left thalamic susceptibility than their male carrier counterparts ($d = 0.35$, $p = 0.042$). Caudal susceptibility differences between men and women non-carriers remained significant after FDR correction ($q < 0.05$).

3.3. Association of EDSS with allele presence

Within progressive MS, C282Y carriers had significantly higher EDSS scores (mean = 5.5, median = 6.0, IQR = 4.0–6.5 vs.

Table 3
Mean magnetic susceptibility (in ppb) of risk allele carriers and non-carriers among relapsing remitting and progressive MS patients.

HFE rs1800562 (C282Y)

	Relapsing			Progressive			Overall p-value
	Non-carrier	Carrier	p-value (*d*)	Non-carrier	Carrier	p-value (*d*)	
T Thalamus							
L Thalamus	− 6.8 (8.4)	− 7.2 (10.9)	0.751 (0.04)	− 9.5 (10.4)	− 14.8 (10.3)	**0.043*** **(0.56)**	0.108
R Thalamus	− 5.5 (8.7)	− 4.6 (9.3)	0.654 (0.10)	− 7.4 (10.2)	− 14.1 (11.3)	**0.007*** **(0.62)**	**0.021***
T Caudate	43.9 (11.7)	41.8 (12.4)	0.384 (0.17)	46.4 (11.7)	45.5 (11.4)	0.803 (0.08)	0.690
L Caudate							
R Caudate							
T Putamen							
L Putamen	48.9 (14.9)	48.3 (14.2)	0.930 (0.04)	52.3 (16.4)	50.2 (13.8)	0.796 (0.14)	0.965
R Putamen	52.2 (15.1)	49.1 (14.0)	0.354 (0.21)	56.3 (17.8)	55.2 (16.8)	0.886 (0.06)	0.788
T Pallidus							
L Pallidus	126.1 (22.9)	121.4 (22.7)	0.299 (0.21)	130.2 (29.3)	132.0 (34.3)	0.777 (0.06)	0.735
R Pallidus	118.0 (24.7)	115.2 (24.2)	0.618 (0.11)	123.0 (29.5)	123.8 (28.2)	0.895 (0.03)	0.954

HFE rs1799945 (H63D)

	Relapsing			Progressive			Overall p-value
	Non-carrier	Carrier	p-value (*d*)	Non-carrier	Carrier	p-value (*d*)	
T Thalamus							
L Thalamus	− 6.2 (8.7)	− 7.6 (8.8)	0.209 (0.16)	− 10.1 (9.5)	− 10.7 (12.4)	0.691 (0.05)	0.298
R Thalamus	− 5.3 (8.1)	− 5.1 (9.6)	0.811 (0.02)	− 7.7 (9.4)	− 9.7 (13.9)	0.265 (0.17)	0.415
T Caudate	43.1 (11.8)	44.7 (11.8)	0.238 (0.14)	46.4 (12.3)	46.5 (10.1)	0.946 (0.01)	0.466
L Caudate							
R Caudate							
T Putamen							
L Putamen	47.3 (13.4)	52.3 (16.4)	**0.013*** (0.33)	52.0 (16.7)	52.9 (14.6)	0.816 (0.06)	0.131
R Putamen	50.6 (14.5)	54.2 (15.4)	0.079 (0.24)	56.2 (18.1)	56.1 (16.5)	0.902 (0.01)	0.425
T Pallidus							
L Pallidus	124.9 (22.7)	125.3 (22.6)	0.862 (0.02)	128.7 (27.8)	135.8 (34.4)	0.200 (0.23)	0.440
R Pallidus	116.7 (25.0)	117.7 (23.0)	0.896 (0.04)	123.5 (29.3)	122.7 (30.7)	0.902 (0.03)	0.939

TF rs1049296 (TF-C2)

	Relapsing			Progressive			Overall p-value
	Non-carrier	Carrier	p-value (*d*)	Non-carrier	Carrier	p-value (*d*)	
T Thalamus							
L Thalamus	− 7.1 (8.9)	− 5.9 (7.6)	0.213 (0.15)	− 10.5 (10.1)	− 9.0 (10.9)	0.523 (0.14)	0.266
R Thalamus	− 5.5 (8.2)	− 4.9 (9.1)	0.535 (0.07)	− 8.3 (10.4)	− 7.9 (10.6)	0.872 (0.04)	0.525
T Caudate	42.8 (11.8)	45.6 (11.1)	0.285 (0.24)	46.4 (11.8)	45.8 (10.1)	0.598 (0.05)	0.511
L Caudate							
R Caudate							
T Putamen							
L Putamen	48.5 (15.2)	49.9 (12.7)	0.616 (0.10)	53.0 (16.6)	51.0 (14.5)	0.617 (0.13)	0.913
R Putamen	51.2 (15.2)	52.8 (13.4)	0.453 (0.11)	56.3 (17.9)	55.9 (16.2)	0.888 (0.02)	0.904
T Pallidus							
L Pallidus	126.5 (23.8)	121.7 (19.9)	0.079 (0.22)	131.2 (30.4)	128.6 (28.6)	0.668 (0.09)	0.410
R Pallidus	118.1 (25.9)	114.9 (21.2)	0.414 (0.14)	124.8 (30.7)	119.3 (25.6)	0.344 (0.19)	0.582

Note: T = Total; L = Left; R = Right. $p < 0.05$ and Cohen's *d* medium effect (> 0.50) are bolded.
Thalamus, putamen and pallidus analyses were carried out separately for the left and right hemisphere due to observed hemispheric differences.
* Remains significant ($p < 0.05$) after adjusting for structural volume.
† Remains significant ($q < 0.05$) after FDR correction by gene.

mean = 6.5, median = 6.5, IQR = 5.75–7.5, p = 0.027). Other genotypes were not correlated with EDSS.

4. Discussion

This is one of the first studies investigating the effects of common genetic variants associated with iron regulation and metabolism (*HFE* C282Y, H63D, and *TF*-C2) on in vivo deep GM measurements in HCs and MS. Of the investigated SNPs, we only observed a higher prevalence of *TF*-C2 in MS patients. Magnetic susceptibility differences between genetic risk carriers vs. non-carriers were mainly observed in our healthy population (with higher susceptibility in the putamen) and progressive MS patients (with lower susceptibility in the thalamus). Interestingly, sex differences were observed not in patients with the risk allele, but among patients with wild-type status.

4.1. Main effects of magnetic susceptibility

As has been extensively reported (Craelius et al., 1982; Zecca et al., 2004; Hagemeier et al., 2012a), deep GM iron levels are thought to be

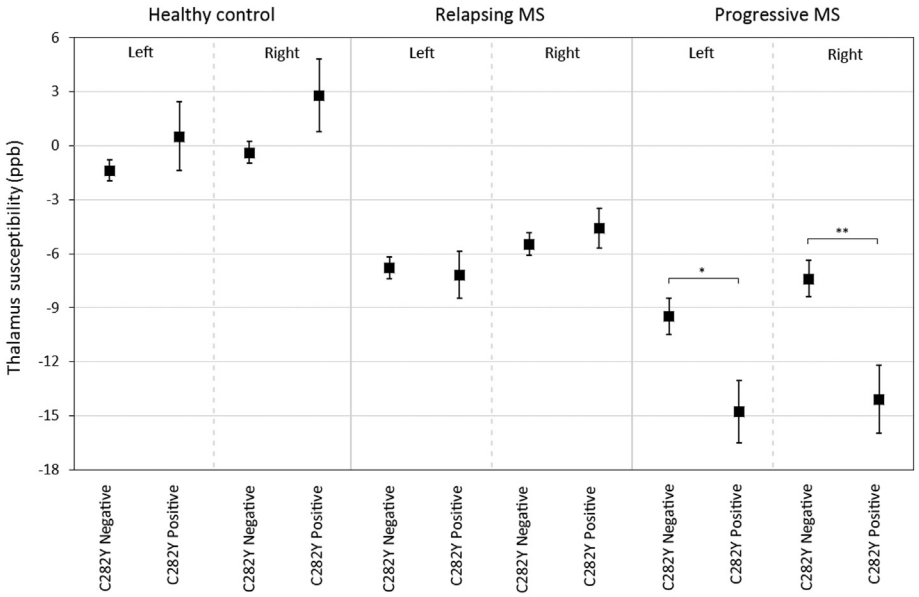

Fig. 2. Distribution of thalamic susceptibility by rs1800562 allele status between HC, RR and Progressive MS. The evolution from HC to RR to progressive MS in thalamic susceptibility reduction is apparent. The C282Y mutation is linked to reduced bilateral thalamus susceptibility within progressive MS. Data is presented as mean ± standard error. *p < 0.05, **p < 0.01.

disturbed in MS. In MS, T_2 hypointensity, R_2*, and susceptibility-weighted phase imaging are correlated with structural damage (Bermel et al., 2005; Zivadinov et al., 2012), advancing MS disease course (Hagemeier et al., 2012b; Blazejewska et al., 2015), and with physical and cognitive measures of disability (Brass et al., 2006; Burgetova et al., 2010; Hagemeier et al., 2013b; Modica et al., 2015). This study used a recently developed advanced MR imaging technique (QSM) (Reichenbach et al., 2015; Schweser et al., 2016), allowing the measurement of subtle changes of the magnetic susceptibility of tissue. QSM is regarded as one of the most sensitive and specific techniques for studying tissue iron in vivo in MS (Langkammer et al., 2013; Stuber et al., 2015).

Although not the primary aim of the present work, in line with previous reports, we observed significant disease group effects in both VBA and ROI analyses: MS patients had higher susceptibility in the caudate, putamen and pallidus compared to controls. Progressive MS patients had higher values in the caudate, right putamen, and left pallidus compared to RRMS. As was recently reported using QSM (Hagemeier et al., 2017; Schweser et al., 2017), thalamic susceptibility was lower in RRMS (vs HC) and progressive patients (vs RRMS). Decreased thalamic iron concentrations are known to occur in normal aging (Hallgren and Sourander, 1958; Hagemeier et al., 2017), and is likely a product of physically reduced iron levels, and in MS, due to myelin changes, and/or potentially even deposition of insoluble calcium phosphate (Schweser et al., 2010, 2011; Hagemeier et al., 2017).

VBA analysis showed the decreased thalamic susceptibility effect to be mostly contained to the pulvinar of the thalamus, a finding opposite to other reports which generally observe increased pulvinar iron levels (e.g. (Hagemeier et al., 2012b; Zivadinov et al., 2012; Al-Radaideh et al., 2013; Rudko et al., 2014)). It may be that increased pulvinar susceptibility is found predominantly in younger patients (< 40 years) whereas in older patients, as is the case in this study, pulvinar susceptibility has decreased below that in controls (Schweser et al., 2017). A reduction in thalamic susceptibility points to a reduction in iron concentration, possibly from iron being released from oligodendrocytes as a result of chronic microglia activation (Zhang et al., 2006).

4.2. Iron genes and magnetic susceptibility in healthy controls

Three SNPs known to be associated with iron disruption were quantified: *HFE* rs1800562 (C282Y) and *HFE* rs1799945 (H63D), associated with hereditary hemochromatosis, and rs1049296 (TF-C2), associated with iron transport. Mutations were observed less frequently in HC than MS, with genotype frequency being highly comparable to other reports. In a large population-based study comprising 5171 subjects (Steinberg et al., 2001), the C282Y genotype had a prevalence of 8.6% (9% in the present study), and H63D had a prevalence of 23.3% (23% in the present study). The *TF*-C2 allele frequency varies widely depending on the population under study, but ranges between 9 and 20% in European samples (Beckman et al., 1998). *TF*-C2 frequency in our study was 17%, with our sample consisting of approximately 80% Caucasians. These findings indicate that the HCs investigated are representative and that observations of deep GM magnetic susceptibility can be generalized to a larger population.

No differences in magnetic susceptibility were observed after correction for FDR. However, without FDR correction, HCs with the H63D mutation had significantly higher right putamen susceptibility than those without. Concurrently, putamen volume was markedly lower in subjects who were H63D carriers. After adjusting for structural volume, right putamen susceptibility remained significantly higher among risk allele carriers ($p < 0.05$). As such, it stands to reason that the H63D gene variant is associated with an increase of iron in the right putamen of HCs. Further unadjusted differences were observed in right putamen susceptibility and volume (C282Y) and thalamus volume (H63D) of HCs. Bartzokis et al. (Bartzokis et al., 2010) has previously revealed significantly higher brain iron in the caudate nucleus of older men (≥ 55 years) who had at least one iron gene mutation. Caudate magnetic susceptibility nor volume reached significance in the present study. Another recent study investigated a range of factors possibly linked to brain iron changes in the normal aging brain using R2*, including genetic predisposition (Pirpamer et al., 2016). In contrast to the present study (where a putamen x gene effect was observed) and Bartzokis et al. (Bartzokis et al., 2010) (where a caudate x gene effect was observed), they did not report any effect of the C282Y, H63D or *TF*-C2 mutation. It has to be noted that, as in Bartzokis et al., Pirpamer et al. report a substantially older sample (mean age: 65.4 years) when compared to the present study (mean age: 45.6 years). Potential gene effects may manifest at different ages, especially considering deep GM iron levels are known change at different trajectories depending on region and age (Hallgren and Sourander, 1958).

4.3. Iron genes and magnetic susceptibility in multiple sclerosis

To our knowledge, this is one of the first studies investigating genes coding for iron functioning in MS in the context of iron-sensitive brain MRI. MS patients with the H63D mutation had increased left putamen

Table 4
Mean magnetic susceptibility (in ppb) of men and women and risk allele carriers and non-carriers among patients with multiple sclerosis.

HFE rs1800562 (C282Y)

	Allele non-carriers			Allele carriers			Overall p-value
	Men	Women (n = 213)	p-value (*d*)	Men (n = 15)	Women	p-value (*d*)	
T Thalamus							
L Thalamus	− 7.7 (8.1)	− 7.9 (9.9)	0.676 (0.02)	− 7.3 (7.5)	− 10.7 (11.8)	0.182 (0.34)	0.259
R Thalamus	− 5.8 (8.2)	− 6.5 (9.8)	0.251 (0.08)	− 4.4 (8.1)	− 9.2 (11.7)	0.105 (0.48)	0.114
T Caudate	48.7 (10.7)	42.8 (11.7)	< **0.001***,† **(0.53)**	44.4 (9.8)	42.3 (13.1)	0.744 (0.18)	**0.001***,†
L Caudate							
R Caudate							
T Putamen							
L Putamen	53.1 (15.8)	48.7 (14.2)	**0.025*** (0.29)	48.0 (14.2)	49.3 (14.0)	0.646 (0.09)	0.152
R Putamen	56.1 (16.7)	52.4 (15.9)	0.061 (0.23)	51.6 (16.6)	50.8 (14.6)	0.938 (0.05)	0.243
T Pallidus							
L Pallidus	128.1 (25.9)	127.3 (25.3)	0.971 (0.03)	116.8 (26.1)	128.5 (27.0)	0.101 (0.44)	0.401
R Pallidus	120.5 (27.3)	119.5 (26.4)	0.862 (0.04)	111.9 (23.4)	120.7 (26.4)	0.162 (0.35)	0.647

HFE rs1799945 (H63D)

	Allele non-carriers			Allele carriers			Overall p-value
	Men	Women	p-value (*d*)	Men	Women	p-value (*d*)	
T Thalamus							
L Thalamus	− 7.6 (7.9)	− 7.8 (9.8)	0.739 (0.02)	− 8.3 (8.3)	− 8.9 (10.9)	0.440 (0.06)	0.641
R Thalamus	− 5.8 (7.9)	− 6.5 (9.1)	0.348 (0.08)	− 5.6 (8.9)	− 7.1 (12.1)	0.204 (0.14)	0.422
T Caudate	48.2 (10.6)	42.2 (12.3)	< **0.001***,† **(0.52)**	48.3 (10.7)	43.6 (11.3)	0.111 (0.43)	**0.001***,†
L Caudate							
R Caudate							
T Putamen							
L Putamen	51.6 (15.1)	47.7 (14.6)	**0.049*** (0.26)	54.3 (16.3)	51.2 (15.6)	0.670 (0.19)	**0.046***
R Putamen	55.7 (17.3)	51.1 (15.4)	**0.027*** (0.28)	55.2 (15.1)	54.6 (16.2)	0.686 (0.04)	0.094
T Pallidus							
L Pallidus	127.6 (25.9)	125.7 (24.2)	0.758 (0.08)	125.7 (26.2)	130.2 (27.7)	0.238 (0.17)	0.425
R Pallidus	121.1 (27.9)	118.3 (26.3)	0.508 (0.10)	115.3 (24.3)	121.4 (25.9)	0.145 (0.36)	0.413

HFE rs1049296 (TF-C2)

	Allele non-carriers			Allele carriers			
	Men	Women	p-value (*d*)	Men	Women	p-value (*d*)	Overall p-value
T Thalamus							
L Thalamus	− 9.2 (7.7)	− 7.8 (10.2)	0.433 (0.15)	− 5.3 (8.0)	− 8.4 (9.6)	**0.042*** (0.35)	0.136
R Thalamus	− 5.9 (7.6)	− 6.8 (9.8)	0.246 (0.10)	− 5.9 (9.1)	− 6.1 (10.3)	0.707 (0.02)	0.623
T Caudate	48.6 (10.8)	41.9 (11.9)	< **0.001***,† **(0.59)**	47.6 (10.5)	43.9 (10.7)	0.129 (0.35)	< **0.001***,†
L Caudate							
R Caudate							
T Putamen							
L Putamen	53.9 (16.6)	48.2 (15.2)	**0.014*** (0.36)	49.5 (12.4)	51.1 (14.1)	0.480 (0.12)	0.070
R Putamen	56.6 (17.3)	51.2 (15.6)	**0.020*** (0.33)	53.5 (14.4)	54.3 (14.6)	0.630 (0.06)	0.100
T Pallidus							
L Pallidus	130.3 (26.5)	127.1 (26.2)	0.539 (0.12)	120.1 (23.5)	127.7 (23.1)	0.068 (0.33)	0.129
R Pallidus	121.8 (29.5)	119.7 (27.1)	0.741 (0.07)	113.9 (19.6)	118.7 (25.2)	0.222 (0.21)	0.452

Note: T = Total; L = Left; R = Right. $p < 0.05$ and Cohen's *d* medium effect (> 0.50) are bolded.
Thalamus, putamen and pallidus analyses were carried out separately for the left and right hemisphere due to observed hemispheric differences.
* Remains significant ($p < 0.05$) after adjusting for volume.
† Remains significant ($p < 0.05$) after FDR correction by gene.

susceptibility (+ 3.2 ppb). No other region showed susceptibility or volume differences between carriers and non-carriers. Subsequent analysis of relapsing and progressive MS patients showed a differing picture for each group. RRMS patients retained the uncorrected effect of H63D in the left putamen that was observed in the MS group as a whole, while progressive patients who had the C282Y gene variant had substantially lower susceptibility in the bilateral thalamus (> − 5.3 ppb, $d > 0.56$), indicating lower thalamic iron. Regardless of genotype, progressive patients had lower thalamic susceptibility than relapsing patients, who in turn had lower susceptibilities than HCs. In line with our study, a recent report found lower thalamic susceptibility in RRMS patients, compared to HCs (Burgetova et al., 2017). They also observed an increase in susceptibility for (primary) progressive MS. This apparent discrepancy may be explained by the present study including secondary-progressive patients and Burgetova's sex ratio being substantially different (female/male: 0.7 vs. 1.8 in the present study).

Few studies have investigated iron associated genetic mutations in MS. Ristic et al. (Ristic et al., 2005) investigated prevalence rates of genes associated with hereditary hemochromatosis and found a similar rate of C282Y and H63D mutations between controls and MS, and did

not observe increased disease progression among carriers. Earlier disease onset in patients carrying the C282Y mutant allele, however, was observed (Ristic et al., 2005). Also, although not statistically significant, EDSS scores were higher in patients heterozygous for H63D (EDSS: 4.7 ± 2.5) and C282Y (EDSS: 5.0 ± 1.8) compared to MS patients with wild-type alleles (EDSS: 4.3 ± 2.4). Rubio et al. (Rubio et al., 2004) reported an increased frequency of the *HFE* C282Y mutation in MS compared to HC (10.2% vs. 6.7%). A more recent study investigating the association of iron related polymorphisms in MS found an increased Multiple Sclerosis Severity Score (MSSS) and disease progression in H63D-, but not among C282Y- carriers (Gemmati et al., 2012). Presence of any iron risk polymorphism under investigation (H63D, C282Y, and others vs. wild-type) was associated with higher EDSS, MSSS, and progression scores. In the present study, mutations in the *HFE* gene (C282Y & H63D) were not significantly more present in MS patients, although frequencies were overall higher. The transferrin mutation (TF-C2) did occur more frequently (29% vs. 17%) in patients. Within progressive MS, only C282Y was associated with higher EDSS scores. This moderate association of EDSS with genotype is in line with Ristic et al. (Ristic et al., 2005). However, we observed no difference in MS disease onset between carriers and non-carriers.

4.4. Iron genes and sex differences in multiple sclerosis

We have previously reported that women had an accelerated putamen susceptibility trajectory over age as compared to men among healthy subjects (Hagemeier et al., 2013a). In contrast to this finding, but in line with the present study, Bartzokis et al. (Bartzokis et al., 1997; Bartzokis et al., 2007) showed increased brain iron in men compared to women and suggested that brain iron levels could contribute to earlier disease onset of neurodegenerative disorders in men. Persson et al. (Persson et al., 2015) reported lower substantia nigra susceptibility in women and a distinct plateauing effect specifically in the pulvinar nucleus of only women. Interestingly, women who were postmenopausal had lower levels of iron deposition, even after adjusting for the effects of aging (Persson et al., 2015). Overall, it appears sex may influence brain iron status due to several factors including sex hormones, menopause and menstruation. The influence of genetic risk factors and sex differences are less clear, however. Bartzokis et al. (Bartzokis et al., 2011) report that the association of brain iron and cognition was influenced by sex and genetic variation independently, i.e. they observed a strong association of (i) verbal memory function and hippocampal iron in men, and (ii) working memory function with basal ganglia iron among solely wild-type *HFE* and *TF* gene carriers, regardless of gender. Evidently, there are specific sex and gene effects regarding deep GM iron levels. In the present study we did not investigate cognitive functioning. However, within MS patients, distinct sex effects were observed in the susceptibility of the caudate and putamen, but, similar to Bartzokis et al., most effects were only apparent in wild-type gene carriers. Female non-carriers presented with lower susceptibilities than men, while average susceptibilities among participants with the C282Y, H63D, or C2 mutation were similar between men and women; with male carriers having the same or lower susceptibilities, and female carriers having higher susceptibilities than their non-risk allele carrying counterparts. One potential explanation could be a group difference between the number of women who have reached menopause. Even though we did not record menopause status among women, female MS patients with genetic mutations were of similar age to those without (mean age 46.0 ± 12.1 vs. 46.4 ± 10.8 years), making a group difference in number of women who are postmenopausal unlikely. Therefore, it may be that specifically within female MS patients, having any of the *HFE* or *TF* risk alleles could increase iron levels to a similar level as men. Our results are in line with the observation that women tend to have lower susceptibilities in the deep GM than men (Bartzokis et al., 2007). Genetic mutations of iron-related genes may be a risk factor for women with respect to brain iron measurements; conversely, being a gene carrier male MS patient may be immaterial or even somewhat protective. Although only indirectly related to this, it is interesting to note that Bathum et al. (Bathum et al., 2001) reported that the C282Y genetic variant frequency reduces with age, suggesting carriers have a decreased life expectancy; this finding was specific to women. In addition, as men with MS tend to have poorer outcomes and progress more rapidly than women (Tremlett et al., 2010), further research into genetic variation among women will have to be conducted to elucidate to what extent disease course is influenced.

4.5. Limitations

Although the frequency of genetic variation is in line with previous reports (Steinberg et al., 2001), some of the investigated study groups were limited in size, especially in the smaller HC sample (e.g. n = 13 C282Y allele carriers in HCs). Further, because of limited sample size we did not investigate any interaction effects of sex with genotype within HCs. While limited statistical power was less of an issue in the MS group, sub-analyses within disease type and sex were carried out using smaller samples. Both unadjusted and adjusted (FDR) p-values are reported to both maximize power and minimize false negative and positive findings. Irrespective of statistical power to detect significance, effect sizes were reported, and VBA analyses were carried out using all participants. Future studies employing larger sample sizes are warranted.

ROI-based analysis was employed in this and many other studies investigating susceptibility in MS. The FSL FIRST method may introduce disease-related anatomical bias due to brain abnormalities, although inaccuracies are likely to stem from poor transformation to MNI space (Feng et al., 2017), suggesting inaccuracies manifest randomly. Furthermore, tissue pathology may be restricted to certain anatomical sub-regions (Schweser et al., 2017), such as the pulvinar, as was observed previously (Zivadinov et al., 2012; Hagemeier et al., 2013c) and in this study using VBA.

Magnetic susceptibility may be influenced by factors other than iron, including changes in myelin or atrophy of tissue compartments with little iron. In the present study, susceptibility values were referenced to the whole brain average susceptibility, whereas several authors have utilized differing reference regions, e.g. the internal capsule (Straub et al., 2017) and frontal deep white matter (Deistung et al., 2013). The choice of reference region has substantial impact on the results due to pathology-related changes in the reference regions. In our view, the whole brain average represents the best trade-off between susceptibility anisotropy effects, localized artifacts, and pathology related susceptibility changes (Hagemeier et al., 2017).

4.6. Conclusion

In conclusion, we sought to investigate whether iron linked genetic polymorphisms were associated with deep GM susceptibility, and thereby may have an influence on brain iron levels. Our findings moderately support this notion: differences were observed between genetic risk allele carriers and non-carriers, although some effects were lost to multiple comparison correction. Increased susceptibility, indicative of higher iron levels, was observed in C282Y and H63D allele carriers in the right putamen of HCs, and left putamen of patients with MS (H63D). Bilateral thalamic iron susceptibility tended to be lower in progressive-, but not relapsing- MS patients with the C282Y mutation. Sex differences were apparent in MS patients; women with wild-type (but not mutation) gene status had lower magnetic susceptibilities than men, suggesting that iron-related risk alleles could be a risk factor for female MS patients. Further inquiry into the interaction of sex and genotype with brain iron is warranted.

Supplementary data to this article can be found online at https://doi.org/10.1016/j.nicl.2017.11.003.

Disclosures

Robert Zivadinov received personal compensation from Teva Pharmaceuticals, Biogen Idec, EMD Serono, Genzyme-Sanofi, Claret Medical, IMS Health and Novartis for speaking and consultant fees. He received financial support for research activities from Teva Pharmaceuticals (CNS-2014-91, CNS-2013-68), Genzyme-Sanofi (GZ-2016-11571, GZ-2014-11225), Novartis (C028-3001838798, C028-300847352), Claret Medical, Intekrin (INT-131) and IMS Health. Dr. Zivadinov serves on editorial board of J Alzh Dis, BMC Med, BMC Neurol, Vein and Lymphatics and Clinical CNS Drugs. He is Executive Director and Treasurer of International Society for Neurovascular Disease.

Bianca Weinstock-Guttman has participated in speaker's bureaus and served as a consultant for Biogen Idec, Teva Neuroscience, EMD Serono, Novartis, Genzyme & Sanofi, and Genentech. Dr. Weinstock-Guttman also has received grant/research support from the agencies listed in the previous sentence. She serves in the editorial board for BMC Neurology, Journal of International MS, Journal of Multiple Sclerosis.

Michael G. Dwyer has received personal compensation from Claret Medical and EMD Serono, and research grant support from Novartis.

Murali Ramanathan has received research funding from the National Multiple Sclerosis Society (RG4836) and the National Science Foundation (1514204). He receives royalty income from a self-published textbook.

Jesper Hagemeier, Ferdinand Schweser, Fuchin Lin and Niels Bergsland have nothing to disclose.

References

Abdul-Rahman, H.S., Gdeisat, M.A., Burton, D.R., Lalor, M.J., Lilley, F., Moore, C.J., 2007. Fast and robust three-dimensional best path phase unwrapping algorithm. Appl. Opt. 46 (26), 6623–6635.

Acosta-Cabronero, J., Williams, G.B., Cardenas-Blanco, A., Arnold, R.J., Lupson, V., Nestor, P.J., 2013. In vivo quantitative susceptibility mapping (QSM) in Alzheimer's disease. PLoS One 8 (11), e81093.

Al-Radaideh, A.M., Wharton, S.J., Lim, S.Y., Tench, C.R., Morgan, P.S., Bowtell, R.W., et al., 2013. Increased iron accumulation occurs in the earliest stages of demyelinating disease: an ultra-high field susceptibility mapping study in Clinically Isolated Syndrome. Mult. Scler. 19 (7), 896–903.

Bakshi, R., Benedict, R.H., Bermel, R.A., Caruthers, S.D., Puli, S.R., Tjoa, C.W., et al., 2002. T2 hypointensity in the deep gray matter of patients with multiple sclerosis: a quantitative magnetic resonance imaging study. Arch. Neurol. 59 (1), 62–68.

Bartzokis, G., Beckson, M., Hance, D.B., Marx, P., Foster, J.A., Marder, S.R., 1997. MR evaluation of age-related increase of brain iron in young adult and older normal males. Magn. Reson. Imaging 15 (1), 29–35.

Bartzokis, G., Tishler, T.A., PH, Lu, Villablanca, P., Altshuler, L.L., Carter, M., et al., 2007. Brain ferritin iron may influence age- and gender-related risks of neurodegeneration. Neurobiol. Aging 28 (3), 414–423.

Bartzokis, G., PH, Lu, Tishler, T.A., Peters, D.G., Kosenko, A., Barrall, K.A., et al., 2010. Prevalent iron metabolism gene variants associated with increased brain ferritin iron in healthy older men. J. Alzheim. Dis. 20 (1), 333–341.

Bartzokis, G., Lu, P.H., Tingus, K., Peters, D.G., Amar, C.P., Tishler, T.A., et al., 2011. Gender and iron genes may modify associations between brain iron and memory in healthy aging. Neuropsychopharmacology 36 (7), 1375–1384.

Bathum, L., Christiansen, L., Nybo, H., Ranberg, K.A., Gaist, D., Jeune, B., et al., 2001. Association of mutations in the hemochromatosis gene with shorter life expectancy. Arch. Intern. Med. 161 (20), 2441–2444.

Beckman, L.E., Van Landeghem, G.F., Sikstrom, C., Beckman, L., 1998. DNA polymorphisms and haplotypes in the human transferrin gene. Hum. Genet. 102 (2), 141–144.

Benjamini, Y., Hochberg, Y., 1995. Controlling the false discovery rate: a practical and powerful approach to multiple testing. J. R. Stat. Soc. 57 (1), 289–300.

Bermel, R.A., Puli, S.R., Rudick, R.A., Weinstock-Guttman, B., Fisher, E., Munschauer 3rd, F.E., et al., 2005. Prediction of longitudinal brain atrophy in multiple sclerosis by gray matter magnetic resonance imaging T2 hypointensity. Arch. Neurol. 62 (9), 1371–1376.

Bettencourt, A., Silva, A.M., Santos, E., Gomes, S., Mendonca, D., Costa, P.P., et al., 2011. HFE gene polymorphisms and severity in Portuguese patients with multiple sclerosis. Eur. J. Neurol. 18 (4), 663–666.

Blazejewska, A.I., Al-Radaideh, A.M., Wharton, S., Lim, S.Y., Bowtell, R.W., Constantinescu, C.S., et al., 2015. Increase in the iron content of the substantia nigra and red nucleus in multiple sclerosis and clinically isolated syndrome: a 7 Tesla MRI study. J. Magn. Reson. Imaging 41 (4), 1065–1070.

Brass, S.D., Benedict, R.H., Weinstock-Guttman, B., Munschauer, F., Bakshi, R., 2006. Cognitive impairment is associated with subcortical magnetic resonance imaging grey matter T2 hypointensity in multiple sclerosis. Mult. Scler. 12 (4), 437–444.

Burgetova, A., Seidl, Z., Krasensky, J., Horakova, D., Vaneckova, M., 2010. Multiple sclerosis and the accumulation of iron in the Basal Ganglia: quantitative assessment of brain iron using MRI t(2) relaxometry. Eur. Neurol. 63 (3), 136–143.

Burgetova, A., Dusek, P., Vaneckova, M., Horakova, D., Langkammer, C., Krasensky, J., et al., 2017. Thalamic iron differentiates primary-progressive and relapsing-remitting multiple sclerosis. Am. J. Neuroradiol. 38 (6), 1079–1086.

Burt, M.J., George, P.M., Upton, J.D., Collett, J.A., Frampton, C.M., Chapman, T.M., et al., 1998. The significance of haemochromatosis gene mutations in the general population: implications for screening. Gut 43 (6), 830–836.

Chen, W., Zhu, W., Kovanlikaya, I., Kovanlikaya, A., Liu, T., Wang, S., et al., 2014. Intracranial calcifications and hemorrhages: characterization with quantitative susceptibility mapping. Radiology 270 (2), 496–505.

Connor, J.R., Menzies, S.L., St Martin, S.M., Mufson, E.J., 1992. A histochemical study of iron, transferrin, and ferritin in Alzheimer's diseased brains. J. Neurosci. Res. 31 (1), 75–83.

Costa-Mallen, P., Gatenby, C., Friend, S., Maravilla, K.R., SC, Hu, Cain, K.C., et al., 2017. Brain iron concentrations in regions of interest and relation with serum iron levels in Parkinson disease. J. Neurol. Sci. 378, 38–44.

Craelius, W., Migdal, M.W., Luessenhop, C.P., Sugar, A., Mihalakis, I., 1982. Iron deposits surrounding multiple sclerosis plaques. Arch. Pathol. Lab. Med. 106 (8), 397–399.

Deistung, A., Schafer, A., Schweser, F., Biedermann, U., Turner, R., Reichenbach, J.R., 2013. Toward in vivo histology: a comparison of quantitative susceptibility mapping (QSM) with magnitude-, phase-, and R2*-imaging at ultra-high magnetic field strength. NeuroImage 65, 299–314.

Dekker, M.C., Giesbergen, P.C., Njajou, O.T., van Swieten, J.C., Hofman, A., Breteler, M.M., et al., 2003. Mutations in the hemochromatosis gene (HFE), Parkinson's disease and parkinsonism. Neurosci. Lett. 348 (2), 117–119.

Farina, M., Avila, D.S., da Rocha, J.B., Aschner, M., 2013. Metals, oxidative stress and neurodegeneration: a focus on iron, manganese and mercury. Neurochem. Int. 62 (5), 575–594.

Feng, X., Deistung, A., Dwyer, M.G., Hagemeier, J., Polak, P., Lebenberg, J., et al., 2017. An improved FSL-FIRST pipeline for subcortical gray matter segmentation to study abnormal brain anatomy using quantitative susceptibility mapping (QSM). Magn. Reson. Imaging 39, 110–122.

Gelineau-Morel, R., Tomassini, V., Jenkinson, M., Johansen-Berg, H., Matthews, P.M., Palace, J., 2012. The effect of hypointense white matter lesions on automated gray matter segmentation in multiple sclerosis. Hum. Brain Mapp. 33 (12), 2802–2814.

Gemmati, D., Zeri, G., Orioli, E., De Gaetano, F.E., Salvi, F., Bartolomei, I., et al., 2012. Polymorphisms in the genes coding for iron binding and transporting proteins are associated with disability, severity, and early progression in multiple sclerosis. BMC Med. Genet. 13, 70.

Groeschel, S., Hagberg, G.E., Schultz, T., Balla, D.Z., Klose, U., Hauser, T.K., et al., 2016. Assessing white matter microstructure in brain regions with different myelin architecture using MRI. PLoS One 11 (11), e0167274.

Hagemeier, J., Geurts, J.J., Zivadinov, R., 2012a. Brain iron accumulation in aging and neurodegenerative disorders. Expert. Rev. Neurother. 12 (12), 1467–1480.

Hagemeier, J., Weinstock-Guttman, B., Bergsland, N., Heininen-Brown, M., Carl, E., Kennedy, C., et al., 2012b. Iron deposition on SWI-filtered phase in the subcortical deep gray matter of patients with clinically isolated syndrome may precede structure-specific atrophy. Am. J. Neuroradiol. 33 (8), 1596–1601.

Hagemeier, J., Dwyer, M.G., Bergsland, N., Schweser, F., Magnano, C.R., Heininen-Brown, M., et al., 2013a. Effect of age on MRI phase behavior in the subcortical deep gray matter of healthy individuals. Am. J. Neuroradiol. 34 (11), 2144–2151.

Hagemeier, J., Weinstock-Guttman, B., Heininen-Brown, M., Poloni, G.U., Bergsland, N., Schirda, C., et al., 2013b. Gray matter SWI-filtered phase and atrophy are linked to disability in MS. Front. Biosci. 5, 525–532.

Hagemeier, J., Yeh, E.A., Brown, M.H., Bergsland, N., Dwyer, M.G., Carl, E., et al., 2013c. Iron content of the pulvinar nucleus of the thalamus is increased in adolescent multiple sclerosis. Mult. Scler. 19 (5), 567–576.

Hagemeier, J., Zivadinov, R., Dwyer, M.G., Polak, P., Bergsland, N., Weinstock-Guttman, B., et al., 2017. Changes of deep gray matter magnetic susceptibility over 2 years in multiple sclerosis and healthy control brain. NeuroImage Clin. http://dx.doi.org/10.1016/j.nicl.2017.04.008. (in press). http://www.sciencedirect.com/science/article/pii/S2213158217300840.

Haider, L., Simeonidou, C., Steinberger, G., Hametner, S., Grigoriadis, N., Deretzi, G., et al., 2014. Multiple sclerosis deep grey matter: the relation between demyelination, neurodegeneration, inflammation and iron. J. Neurol. Neurosurg. Psychiatry 85 (12), 1386–1395.

Hallgren, B., Sourander, P., 1958. The effect of age on the non-haemin iron in the human brain. J. Neurochem. 3 (1), 41–51.

Hanspach, J., Dwyer, M.G., Bergsland, N.P., Feng, X., Hagemeier, J., Bertolino, N., et al., 2017. Methods for the computation of templates from quantitative magnetic susceptibility maps (QSM): Toward improved atlas- and voxel-based analyses (VBA). J. Magn. Reson. Imaging 46 (5), 1474–1484. http://dx.doi.org/10.1002/jmri.25671.

Jellinger, K., Paulus, W., Grundke-Iqbal, I., Riederer, P., Youdim, M.B., 1990. Brain iron and ferritin in Parkinson's and Alzheimer's diseases. J. Neural. Transm. Park. Dis. Dement. Sect. 2 (4), 327–340.

Kappus, N., Weinstock-Guttman, B., Hagemeier, J., Kennedy, C., Melia, R., Carl, E., et al., 2016. Cardiovascular risk factors are associated with increased lesion burden and brain atrophy in multiple sclerosis. J. Neurol. Neurosurg. Psychiatry 87 (2), 181–187.

Kurtzke, J.F., 1983. Rating neurologic impairment in multiple sclerosis: an expanded disability status scale (EDSS). Neurology 33 (11), 1444–1452.

Langkammer, C., Schweser, F., Krebs, N., Deistung, A., Goessler, W., Scheurer, E., et al., 2012. Quantitative susceptibility mapping (QSM) as a means to measure brain iron?

A post mortem validation study. NeuroImage 62 (3), 1593–1599.
Langkammer, C., Liu, T., Khalil, M., Enzinger, C., Jehna, M., Fuchs, S., et al., 2013. Quantitative susceptibility mapping in multiple sclerosis. Radiology 267 (2), 551–559.
Mehta, V., Pei, W., Yang, G., Li, S., Swamy, E., Boster, A., et al., 2013. Iron is a sensitive biomarker for inflammation in multiple sclerosis lesions. PLoS One 8 (3), e57573.
Moalem, S., Percy, M.E., Andrews, D.F., Kruck, T.P., Wong, S., Dalton, A.J., et al., 2000. Are hereditary hemochromatosis mutations involved in Alzheimer disease? Am. J. Med. Genet. 93 (1), 58–66.
Modica, C.M., Zivadinov, R., Dwyer, M.G., Bergsland, N., Weeks, A.R., Benedict, R.H., 2015. Iron and volume in the deep gray matter: association with cognitive impairment in multiple sclerosis. Am. J. Neuroradiol. 36 (1), 57–62.
Patenaude, B., Smith, S.M., Kennedy, D.N., Jenkinson, M.A., 2011. Bayesian model of shape and appearance for subcortical brain segmentation. NeuroImage 56 (3), 907–922.
Persson, N., Wu, J., Zhang, Q., Liu, T., Shen, J., Bao, R., et al., 2015. Age and sex related differences in subcortical brain iron concentrations among healthy adults. NeuroImage 122, 385–398.
Pirpamer, L., Hofer, E., Gesierich, B., De Guio, F., Freudenberger, P., Seiler, S., et al., 2016. Determinants of iron accumulation in the normal aging brain. Neurobiol. Aging 43, 149–155.
Polak, P., Zivadinov, R., Schweser, F., 2015. Gradient unwarping for phase imaging reconstruction. Proc. Int. Soc. Magn. Reson. Med. 2015, p3736.
Polman, C.H., Reingold, S.C., Banwell, B., Clanet, M., Cohen, J.A., Filippi, M., et al., 2011. Diagnostic criteria for multiple sclerosis: 2010 revisions to the McDonald criteria. Ann. Neurol. 69 (2), 292–302.
Reichenbach, J.R., Schweser, F., Serres, B., Deistung, A., 2015. Quantitative susceptibility mapping: concepts and applications. Clin. Neuroradiol. 25 (Suppl. 2), 225–230.
van Rensburg, S.J., Carstens, M.E., Potocnik, F.C., Aucamp, A.K., Taljaard, J.J., 1993. Increased frequency of the transferrin C2 subtype in Alzheimer's disease. Neuroreport 4 (11), 1269–1271.
Ristic, S., Lovrecic, L., Brajenovic-Milic, B., Starcevic-Cizmarevic, N., Jazbec, S.S., Sepcic, J., et al., 2005. Mutations in the hemochromatosis gene (HFE) and multiple sclerosis. Neurosci. Lett. 383 (3), 301–304.
Rouault, T.A., 2013. Iron metabolism in the CNS: implications for neurodegenerative diseases. Nat. Rev. Neurosci. 14 (8), 551–564.
Rubio, J.P., Bahlo, M., Tubridy, N., Stankovich, J., Burfoot, R., Butzkueven, H., et al., 2004. Extended haplotype analysis in the HLA complex reveals an increased frequency of the HFE-C282Y mutation in individuals with multiple sclerosis. Hum. Genet. 114 (6), 573–580.
Rudko, D.A., Solovey, I., Gati, J.S., Kremenchutzky, M., Menon, R.S., 2014. Multiple sclerosis: improved identification of disease-relevant changes in gray and white matter by using susceptibility-based MR imaging. Radiology 272 (3), 851–864.
Sampietro, M., Caputo, L., Casatta, A., Meregalli, M., Pellagatti, A., Tagliabue, J., et al., 2001. The hemochromatosis gene affects the age of onset of sporadic Alzheimer's disease. Neurobiol. Aging 22 (4), 563–568.
Schweser, F., Deistung, A., Lehr, B.W., Reichenbach, J.R., 2010. Differentiation between diamagnetic and paramagnetic cerebral lesions based on magnetic susceptibility mapping. Med. Phys. 37 (10), 5165–5178.
Schweser, F., Deistung, A., Lehr, B.W., Reichenbach, J.R., 2011. Quantitative imaging of intrinsic magnetic tissue properties using MRI signal phase: an approach to in vivo brain iron metabolism? NeuroImage 54 (4), 2789–2807.
Schweser, F., Sommer, K., Deistung, A., Reichenbach, J.R., 2012. Quantitative susceptibility mapping for investigating subtle susceptibility variations in the human brain. NeuroImage 62 (3), 2083–2100.
Schweser, F., Deistung, A., Reichenbach, J.R., 2016. Foundations of MRI phase imaging and processing for Quantitative Susceptibility Mapping (QSM). Z. Med. Phys. 26 (1), 6–34.
Schweser, F., Martins, A., Lin, F., Hagemeier, J., Hanspach, J., Weinstock-Guttman, B., et al., 2017. Decreasing magnetic susceptibility (QSM) of thalamic nuclei in Multiple Sclerosis (MS) – the thalamus as a target of projected inflammation? Proc. Int. Soc. Magn. Reson. Med. p2909.
Smith, S.M., Zhang, Y., Jenkinson, M., Chen, J., Matthews, P.M., Federico, A., De Stefano, N., 2002. Accurate, robust and automated longitudinal and cross-sectional brain change analysis. NeuroImage 17 (1), 479–489.
Stankiewicz, J.M., Neema, M., Ceccarelli, A., 2014. Iron and multiple sclerosis. Neurobiol. Aging 35 (Suppl. 2), S51–8.
Steinberg, K.K., Cogswell, M.E., Chang, J.C., Caudill, S.P., McQuillan, G.M., Bowman, B.A., et al., 2001. Prevalence of C282Y and H63D mutations in the hemochromatosis (HFE) gene in the United States. JAMA 285 (17), 2216–2222.
Straub, S., Schneider, T.M., Emmerich, J., Freitag, M.T., Ziener, C.H., Schlemmer, H.P., et al., 2017. Suitable reference tissues for quantitative susceptibility mapping of the brain. Magn. Reson. Med. 78 (1), 204–214. http://dx.doi.org/10.1002/mrm.26369.
Stuber, C., Morawski, M., Schafer, A., Labadie, C., Wahnert, M., Leuze, C., et al., 2014. Myelin and iron concentration in the human brain: a quantitative study of MRI contrast. NeuroImage 93 (Pt 1), 95–106.
Stuber, C., Pitt, D., Wang, Y., 2015. Iron in multiple sclerosis and its noninvasive imaging with quantitative susceptibility mapping. Int. J. Mol. Sci. 17 (1).
Tremlett, H., Zhao, Y., Rieckmann, P., Hutchinson, M., 2010. New perspectives in the natural history of multiple sclerosis. Neurology 74 (24), 2004–2015.
Wang, X.S., Lee, S., Simmons, Z., Boyer, P., Scott, K., Liu, W., et al., 2004. Increased incidence of the Hfe mutation in amyotrophic lateral sclerosis and related cellular consequences. J. Neurol. Sci. 227 (1), 27–33.
Ward, R.J., Zucca, F.A., Duyn, J.H., Crichton, R.R., Zecca, L., 2014. The role of iron in brain ageing and neurodegenerative disorders. Lancet Neurol. 13 (10), 1045–1060.
Winkler, A.M., Ridgway, G.R., Webster, M.A., Smith, S.M., Nichols, T.E., 2014. Permutation inference for the general linear model. NeuroImage 92, 381–397.
Wu, B., Li, W., Guidon, A., Liu, C., 2012. Whole brain susceptibility mapping using compressed sensing. Magn. Reson. Med. 67 (1), 137–147.
Zecca, L., Youdim, M.B., Riederer, P., Connor, J.R., Crichton, R.R., 2004. Iron, brain ageing and neurodegenerative disorders. Nat. Rev. Neurosci. 5 (11), 863–873.
Zhang, X., Surguladze, N., Slagle-Webb, B., Cozzi, A., Connor, J.R., 2006. Cellular iron status influences the functional relationship between microglia and oligodendrocytes. Glia 54 (8), 795–804.
Zhang, Y., Gauthier, S.A., Gupta, A., Comunale, J., Chia-Yi Chiang, G., Zhou, D., et al., 2016. Longitudinal change in magnetic susceptibility of new enhanced multiple sclerosis (MS) lesions measured on serial quantitative susceptibility mapping (QSM). J. Magn. Reson. Imaging 44 (2), 426–432.
Zivadinov, R., Heininen-Brown, M., Schirda, C.V., Poloni, G.U., Bergsland, N., Magnano, C.R., et al., 2012. Abnormal subcortical deep-gray matter susceptibility-weighted imaging filtered phase measurements in patients with multiple sclerosis: a case-control study. NeuroImage 59 (1), 331–339.
Zivadinov, R., Ramasamy, D.P., Benedict, R.R., Polak, P., Hagemeier, J., Magnano, C., et al., 2016. Cerebral microbleeds in multiple sclerosis evaluated on susceptibility-weighted images and quantitative susceptibility maps: a case-control study. Radiology 281 (3), 884–895.